

Scattering of electrons from acetaldehyde and acetone

Czesław Szmytkowski

Atomic Physics Group, Department of Atomic Physics and Luminescence, Faculty of Applied Physics and Mathematics, Gdańsk University of Technology, 80-233 Gdańsk, Poland

E-mail: czsz@mif.pg.gda.pl

Received 11 September 2009, in final form 17 December 2009

Published 3 February 2010

Online at stacks.iop.org/JPhysB/43/055201

Abstract

Absolute total cross sections (TCSs) for electron scattering from acetaldehyde [(CH₃)CHO] and acetone [(CH₃)₂CO] molecules have been measured at electron-impact energy extending from 0.7 to 400 eV, using a linear electron-transmission technique. The shape of obtained TCS energy dependences appears typical for targets of high electric dipole moment; both TCSs decrease with the energy increase; only between 4 and 12 eV is a weak enhancement in TCSs is clearly perceptible. The experimental TCSs for (CH₃)CHO and for (CH₃)₂CO are also compared with those for their cyclic isomeric counterparts: c-(CH₂)₂O and c-(CH₂)₃O, respectively.

(Some figures in this article are in colour only in the electronic version)

1. Introduction

Comprehensive sets of reliable quantitative electron-scattering measurables allow for modelling reactions involved in plasma-assisted technologies, the deposition of energy by radiation in living cells and processes in interstellar or environmental media (see Christophorou and Olthoff 2004, Sanche 2005, Greenberg 2002, Field 2005 and references therein). In spite of their fundamental and applied importance, data on electron-molecule scattering, though more and more numerous (cf Itikawa 2000–2003), still remain fragmentary and/or are presented in relative units only.

Experimental studies on the electron-assisted processes involving acetaldehyde or acetone molecules in the gas phase are quite abundant. In early experiments, normalized cross sections for electron-impact ionization (ICSs) of acetaldehyde and acetone have been measured at 75 eV by Otvos and Stevenson (1956), Harrison *et al* (1966) and Beran and Kevan (1969), while recently Bull and Harland (2008) obtained the absolute ICSs from 15 to 285 eV. The temporary negative ion formation by electron attachment to acetaldehyde and acetone has been investigated first by Dorman (1966), next by Naff *et al* (1972) and by Jordan and Burrow (1978); more recently, Dressler and Allan (1985, 1986) carried out a high-resolution study on acetaldehyde only. A series of experiments concern the electron-induced excitation of both acetaldehyde and acetone molecules (Naff *et al* 1972, Staley

et al 1975, van Veen *et al* 1976, Benoit *et al* 1987). For acetaldehyde alone, such studies have been performed by Tam and Brion (1974), Dressler and Allan (1985) and Walzl *et al* (1987), while for acetone by e.g. Huebner *et al* (1973) and very recently by Kato *et al* (2009). However, the intensities of the aforementioned phenomena, except cross sections for ionization and for dissociative electron attachment with CH₃⁻ formation (Dressler and Allan 1985), were obtained only in relative units, which alone makes difficult their application for modelling of electron-driven processes or comparison with theoretical computations. The momentum transfer cross section, at thermal electron energy, has been reported for both targets by Garrett (1972) based on swarm experiments of Crawford *et al* (1967), Stockdale *et al* (1967) and Christophorou and Christodoulides (1969). More recently, in the electron-transmission experiment, Kimura *et al* (2000) determined the normalized total cross section for acetone, from 0.8 to 600 eV. In the literature, one can also find experiments concerned with the electron diffraction study of the (CH₃)CHO and (CH₃)₂CO molecular structure (Kato *et al* 1969).

The main purpose of the present work is to provide absolute values of total cross sections (TCSs) describing electron-acetaldehyde and electron-acetone scattering over impact energies from low (0.7 eV) to intermediates (400 eV). Comparison of electron-scattering TCSs for these carbonyl compounds may show how replacing one hydrogen atom in (CH₃)CHO by the methyl group, to form (CH₃)₂CO,

influences electron interaction with molecules (*substitutional effect*). In addition, to examine how the arrangement of atoms in the target molecule reflects in the TCS energy behaviour (*isomer effect*), the current TCS results for the open-chain $(\text{CH}_3)\text{CHO}$ and $(\text{CH}_3)_2\text{CO}$ molecules will be confronted with the recent TCS data (Szymtkowski *et al* 2008, 2009) for their isomeric ring counterparts $\text{c}-(\text{CH}_2)_2\text{O}$ and $\text{c}-(\text{CH}_2)_3\text{O}$ respectively.

2. Methods and procedures

2.1. Experimental

The absolute electron-scattering total cross sections (TCSs) reported in this work were measured from low to intermediate energies using the electron transmission (ET) technique in a linear configuration under single-collision conditions. In the ET method the $\text{TCS}(E)$ is related to the transparency of the target of a density n for an electron beam of given energy E based on the Bouguer-de Beer–Lambert (BBL) relationship

$$\text{TCS}(E) = \frac{1}{nL} \ln \frac{I_0(E)}{I_n(E)},$$

where $I_0(E)$ and $I_n(E)$ are the intensities of the electron beam transmitted through the scattering cell in the absence and presence of the target, respectively; the density $n = p/k\sqrt{T_r T_m}$ is obtained from the ideal gas law using the absolute measurements of the gas target pressure (p), the temperatures of the target cell (T_r) and the MKS capacitance manometer head ($T_m = 322 \text{ K} > T_r$), while the thermal transpiration effect has been taken into account (Knudsen 1910); L is the length of the electron pathway within the target—equal to the distance ($=30.5 \text{ mm}$) between entrance and exit cell apertures; k is the Boltzmann constant.

The instrumentation and procedure employed in the present experiment have already been described previously (e.g. Szymtkowski *et al* 1997, Domaracka *et al* 2006); therefore, only a brief summary is given here. An incident electron beam of required energy E is produced by 127° electrostatic cylindrical monochromator coupled to an electron gun and electrostatic lenses. Then the nearly mono-energetic electron beam ($\Delta E \leq 0.1 \text{ eV}$, fwhm) collides with a static vapour sample of interest in the reaction cell and the electrons getting away from the scattering volume through the exit aperture are energy-discriminated by a retarding field (RF) analyser and eventually are collected by a Faraday cup. The RF analyser enables to discriminate electrons with a kinetic energy difference of 0.1 eV in the case of low-impact energies and about 0.5 eV at intermediates and reduces the number of inelastically scattered electrons which might be accepted by the collector. The electron energy scale is calibrated against the well-known resonant oscillatory structure in the electron current transmitted through N_2 , observed around 2.3 eV . To keep the conditions in the electron optics volume invariable throughout the experiment, irrespective of whether the target is present or absent in the scattering cell, the target vapour is supplied alternately into the cell or into the cell environment, so the residual target pressure in the electron optics region is practically constant, below $80 \mu\text{Pa}$. An intensity of the

ambient magnetic field is reduced to less than 100 nT along the electron trajectory. The samples of acetaldehyde and acetone—commercially supplied by Sigma Aldrich with stated purities better than 99.5% and 99.9% , respectively—were used after repeated vacuum distillation.

The quantities necessary for TCS derivation are taken directly in the experiment, so the obtained TCS is in absolute scale. The final TCS value at each given electron-impact energy, reported in this work, is a weighted mean of results from several series (4–9), each containing up to ten individual runs, performed at a variety of target pressure in the cell, p , from 40 to 140 mPa . The statistical uncertainty (one standard deviation of the weighted mean value) of the resulting absolute TCS does not exceed 1% over the whole energy range used. Typically, the main contribution to the systematic uncertainty in the ET experiments arises from inability to discriminate against electrons which are scattered elastically through small angles in the forward direction; these electrons contribute to the transmitted current $I_n(E)$ and lower the reported TCSs by $5\text{--}7\%$ around the low and high extremes of applied energies, and by about $2\text{--}3\%$ between 5 and 100 eV . The above estimations—due to lack in the literature of measurements and/or calculations on the electron-scattering differential cross sections (DCSs) for acetaldehyde and acetone—are based on the available DCSs for H_2O (e.g. Silva *et al* 2008, Machado *et al* 2005) scaled due to difference in the electric dipole moments of water molecule and targets under study. Additionally, below 2 eV , where the measured TCSs appear to be a steep function of energy, the extra error of $2\text{--}6\%$ arises due to uncertainty in the energy scale. Possible TCS systematic error components, related to measurements of other quantities in the BBL formula, are estimated to be less than 1% each. The overall TCS error, evaluated as a quadrature sum of the statistical and all relevant individual potential systematic uncertainties, amounts to 10% around 1 eV , decreasing to $4\text{--}5\%$ between 3 and 50 eV and increasing again to $6\text{--}7\%$ at the highest applied energies.

3. Results and discussion

In this section, the absolute total electron-scattering cross sections (TCSs) for the acetaldehyde $[(\text{CH}_3)\text{CHO}]$ and for acetone $[(\text{CH}_3)_2\text{CO}]$ molecules are presented. The TCSs were measured in the transmission experiment over a fairly broad range of impact energies from low to intermediates. The numerical TCS values for acetaldehyde and acetone are listed in tables 1 and 2, respectively. Next, we compare TCS energy dependences for both targets under study to examine how the substitution of the hydrogen atom (bonded to the C-atom of the carbonyl group) by the methyl group influences the electron–molecule interaction (*substitutional effect*). Finally, the results for the open-chain $(\text{CH}_3)\text{CHO}$ and $(\text{CH}_3)_2\text{CO}$ molecules are compared to TCS curves for their cyclic counterparts $\text{c}-(\text{CH}_2)_2\text{O}$ and $\text{c}-(\text{CH}_2)_3\text{O}$ respectively, and the *isomeric effect* is indicated.

Table 1. Absolute experimental electron-scattering total cross sections for (CH₃)CHO molecules, in units of 10⁻²⁰ m².

E (eV)	TCS	E (eV)	TCS	E (eV)	TCS	E (eV)	TCS	E (eV)	TCS
0.7	98.5	2.5	46.1	6.5	46.6	20	32.3	100	19.8
0.8	90.5	2.8	45.6	7.0	46.7	22	31.7	110	19.1
0.9	83.1	3.0	45.1	7.5	47.2	25	30.8	120	18.0
1.0	77.2	3.3	44.8	8.0	47.6	27	30.3	140	16.9
1.1	71.4	3.5	44.6	8.5	47.4	30	29.7	160	15.2
1.2	66.7	3.8	44.6	9.0	46.7	35	28.8	180	14.4
1.3	62.8	4.0	44.7	9.5	45.7	40	27.8	200	13.4
1.4	59.1	4.3	44.9	10	44.2	45	26.4	220	12.3
1.5	56.3	4.5	45.2	11	41.1	50	25.7	250	11.4
1.7	52.4	4.8	45.5	12	39.1	60	24.2	275	10.7
1.9	50.0	5.0	46.2	14	36.9	70	23.0	300	10.0
2.1	48.1	5.5	46.8	16	35.3	80	21.8	350	8.92
2.3	47.0	6.0	47.0	18	33.4	90	20.7	400	7.99

Table 2. Absolute experimental electron-scattering total cross sections for (CH₃)₂CO molecules, in units of 10⁻²⁰ m².

E (eV)	TCS	E (eV)	TCS	E (eV)	TCS	E (eV)	TCS	E (eV)	TCS
0.7	126	2.3	54.5	7.0	57.6	18	44.1	90	27.8
0.8	117	2.5	53.2	7.5	58.5	20	42.8	100	26.0
0.9	109	2.8	52.4	8.0	58.8	22	42.0	110	24.7
1.0	100	3.0	52.1	8.5	59.1	25	41.2	120	23.6
1.1	93.0	3.3	52.1	9.0	59.0	27	40.4	140	21.6
1.2	86.6	3.5	52.3	9.5	57.8	30	38.9	160	20.1
1.3	82.2	3.8	52.6	10.0	56.1	35	37.2	180	18.4
1.4	78.3	4.0	52.7	10.5	54.7	40	36.3	200	16.9
1.5	74.9	4.5	53.6	11	53.6	45	35.1	220	15.8
1.6	71.0	5.0	55.1	12	52.2	50	34.4	250	14.6
1.7	67.6	5.5	56.4	13	50.9	60	33.2	300	13.0
1.8	64.4	6.0	56.8	14	48.9	70	31.0	350	11.8
1.9	60.9	6.5	57.7	16	45.8	80	29.5	400	11.0
2.1	56.6								

3.1. Acetaldehyde (CH₃)CHO

Figure 1 shows our absolute TCS for electron scattering by the acetaldehyde molecule as a function of energy, between 0.7 and 400 eV. Considering the energy dependence, the TCS for acetaldehyde generally falls steadily with increasing energy over almost whole energy range investigated; only between 4 and 12 eV the TCS reveals a weak enhancement.

At the lowest applied energies the TCS decreases steeply, from nearly 100 × 10⁻²⁰ m² around 0.7 eV to about 50 × 10⁻²⁰ m² at 2 eV. Such a low-energy TCS behaviour is a characteristic typical of highly polar molecules and can be explained in terms of very long-range electron-dipole interaction (Altshuler 1957); the acetaldehyde molecule possesses the permanent electric dipole moment $\mu = 2.72$ D (Lide 1995–1996). It is worth noting that our TCS energy dependence below 2 eV tends to the momentum transfer cross section at thermal energy ($\sim 6 \times 10^{-17}$ m², see Garrett 1972); although, this value seems to be overestimated.

In the vicinity of 3.6 eV, the TCS curve has a shallow minimum of about 45 × 10⁻²⁰ m², while above 4 eV the TCS increases slowly to almost 48 × 10⁻²⁰ m² around 8 eV. More thorough inspection of the TCS curve within 4–12 eV energy range suggests that the visible broad enhancement might be composed of two weak humps, the first centred near 6 eV and the second one peaked at 8 eV, superimposed on the

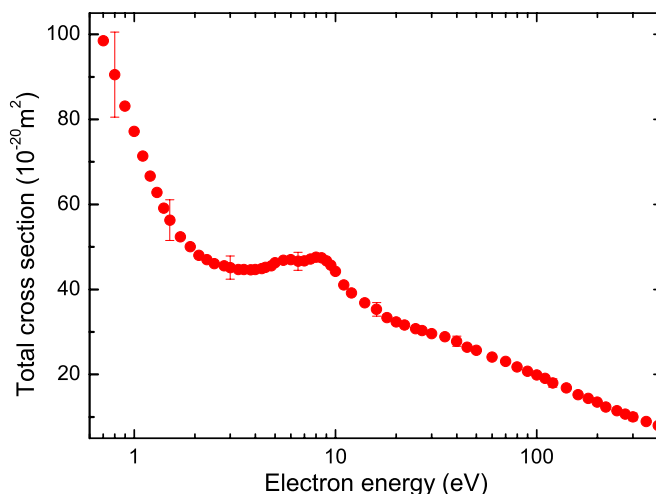


Figure 1. Experimental total cross sections for electron scattering from (CH₃)CHO molecules: (●), present; error bars represent overall, systematic plus statistical, uncertainties.

weak smooth background. The 4–12 eV enhancement may correspond to numerous electron-scattering effects already observed in early experiments. In this energy region, Dorman (1966), Naff *et al* (1972) and Dressler and Allan (1985, 1986) identified various negative fragments of the acetaldehyde

Table 3. Parameters of C_2H_4O and C_3H_6O compounds: permanent electric dipole moment (μ), electrical polarizability (α) and the gas-kinetic collisional cross section (σ_{gk}), from Lide (1995–1996) if not indicated.

Molecule	μ (Debye)	α (10^{-30} m^3)	σ_{gk} (10^{-20} m^2)
$(CH_3)CHO$	2.72	4.6	14–15 ^a
$(CH_3)_2CO$	2.88	6.4	18.6 ^b
$c\text{-(}CH_2\text{)}_2O$	1.89	4.4	11.2 ^b
$c\text{-(}CH_2\text{)}_3O$	1.94	6.1 ^c	13–14 ^d

^a Present work.

^b Estimated from van der Waals constant b (Lide 1995–1996).

^c Estimation based on the additivity formula (Miller 1990).

^d From Szmytkowski *et al* (2009).

molecule. These anions result from the dissociation of the temporary negative compound states (resonances) formed after the impinging electron attaches to the target molecule. The dissociative attachment cross section for the CH_3^- anion formation, estimated by Dressler and Allan (1985), is of the order of 10^{-23} m^2 , within the energy range 6.3–7 eV. In the high-resolution dissociative spectra, Dressler and Allan (1985, 1986) revealed formation of two Feshbach resonances, at 6.3 and 6.6 eV, and two shape resonances, near 8 and 10 eV. Feshbach resonances were also responsible for very weak structures perceived between 6 and 7.2 eV by Dressler and Allan (1986) in the electron-transmission spectrum. Their study on the vibrational excitation of acetaldehyde also indicates the presence of another broad shape resonance located at 6.8 eV. Electron excitation spectra (Naff *et al* 1972, Tam and Brion 1974, Staley *et al* 1975, van Veen *et al* 1976, Dressler and Allan 1986 and Walzl *et al* 1987) yield information on numerous electronic transitions in the 4–10 eV energy range. Although, the above-mentioned effects each alone seem to be rather weak, their superposition may result in the observed broad weak TCS enhancement.

At electron energies beyond 9 eV, the TCS decreases continuously with energy down to $8 \times 10^{-20} \text{ m}^2$ at 400 eV. Worth noting is also the very broad shoulder in the TCS curve visible within the range 20–50 eV. An origin of this feature may be related, in part, to the presence of numerous weak resonances in this energy region; it may also arise due to direct electron-induced processes allowed at these energies, especially the ionization; the ionization cross section in its maximum near 90 eV amounts to $6.7 \times 10^{-20} \text{ m}^2$ (Bull and Harland 2008). Based on our systematic TCS measurements we have noted that there is a correlation between the electron-scattering TCS at intermediate energies and a gas-kinetic cross section for respective molecule; the estimated $\sigma_{gk} = 14\text{--}15 \times 10^{-20} \text{ m}^2$ for acetaldehyde is presented in table 3 and compared to σ_{gk} values for some oxygen-containing hydrocarbon molecules.

3.2. Acetone ($CH_3)_2CO$

Total electron-scattering cross sections measured for acetone are presented in figure 2, from 0.7 to 400 eV. The current absolute TCS results are compared with the only available

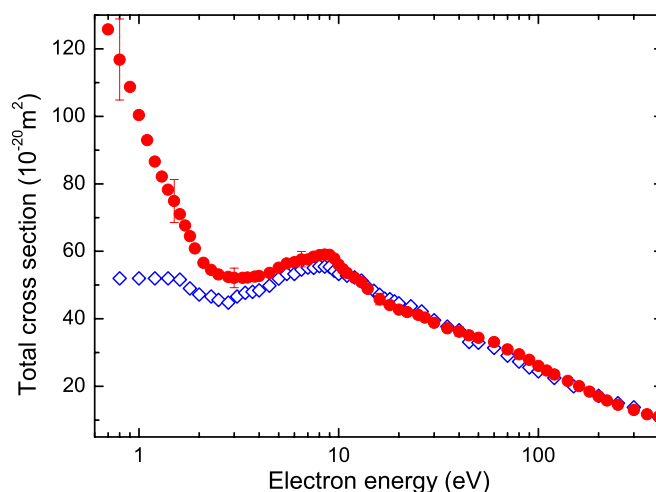


Figure 2. Experimental total cross sections (TCSs) for electron scattering from $(CH_3)_2CO$: (●), present, absolute, error bars represent overall uncertainties; (◇), Kimura *et al* (2000), normalized.

TCS normalized data of Kimura *et al* (2000) at overlapping energies. Reasonable general agreement, especially with respect to the shape, is observed between the present and the earlier TCS curve at energies above 2 eV, while a substantial deviation is observed at the lowest applied energies. Up to 100 eV the compared TCSs fluctuate one over each other: our measurements between 2 and 10 eV lay 6–11% above Kimura *et al* results; fall off (2–4%) below their points within 12–40 eV; then rise slightly and above 100 eV both measured TCSs converge. From 0.8 to 2 eV, the data of Kimura *et al* (2000) are nearly constant and stay well below the present TCS which raises steeply towards lower energies. Such a serious disagreement between the low-energy TCSs ($\sim 100\%$ around 1 eV) is somewhat confusing. There are, however, two arguments which suggest that the present low-energy TCS seems to be realistic: (i) the cross section derived at thermal energies by Christophorou and Christodoulides (1969) amounts to $3 \times 10^{-17} \text{ m}^2$ and smoothly extrapolates our low-energy curve; (ii) the $(CH_3)_2CO$ molecule possesses the high permanent electrical dipole moment ($=2.88 \text{ D}$, Lide 1995–1996) what usually reflects in a very steep increase of TCS towards zero energy. Generally, the present TCS energy dependence for acetone closely resembles TCS energy functions for strongly polar molecules, e.g. for H_2O (cf Szmytkowski and Mozejko 2006). It decreases with increasing impact energy, from about $126 \times 10^{-20} \text{ m}^2$ near 0.7 eV down to $11 \times 10^{-20} \text{ m}^2$ at the highest applied energy, 400 eV. However, some weak features in the TCS curve are discernible and worth noting.

Figure 2 shows a weak local minimum of $52 \times 10^{-20} \text{ m}^2$ around 3.1 eV followed by a broad enhancement spanned within 4–12 eV and peaked near 8.5 eV ($59 \times 10^{-20} \text{ m}^2$). This broad feature may be related to resonant scattering via formation of temporary negative ion states as well as to direct inelastic processes allowed in this energy range. A suggestion on the resonant contribution to the enhancement comes from the experiment of Dorman (1966), in

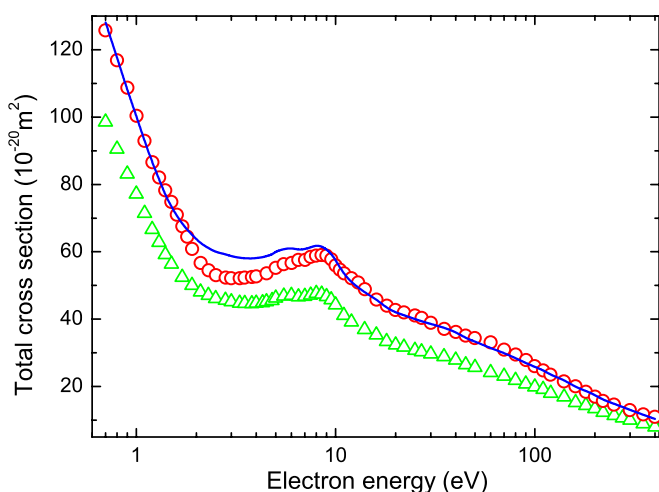


Figure 3. Comparison of total absolute cross sections (TCSs) for electron scattering from carbonyl compounds: $(\text{CH}_3)_2\text{CO}$, (\bullet), present; $(\text{CH}_3)\text{CHO}$, (Δ), present. To demonstrate the similarity in the shape of compared TCSs, the TCS for acetaldehyde is multiplied by 1.3 (—).

which he recorded various negative-ion fragments of acetone in the vicinity of 9 eV. Based on the electron-impact excitation spectra taken within 4–9 eV, Naff *et al* (1972), Staley *et al* (1975) and van Veen *et al* (1976) revealed numerous electronic transitions in the acetone molecule.

On the descending part of the TCS energy function, in the 13–18 eV and 30–90 eV ranges, some weak shoulders are easily discernible. Very recent experiment of Kato *et al* (2009), on the electron-induced C=O stretching excitation, indicates that the feature around 17 eV may be attributed to the formation of a shape resonant state. The shoulder centred near 70 eV is most probably associated with the electron-induced ionization of molecule; the electron-impact ionization cross section for acetone (Bull and Harland 2008) has a flat maximum around 100 eV of $9 \times 10^{-20} \text{ m}^2$.

3.3. Comparison of electron-scattering TCSs for $(\text{CH}_3)\text{CHO}$ and $(\text{CH}_3)_2\text{CO}$ molecules: substitutional effect

In figure 3, the TCS for electron scattering from the acetaldehyde molecule is compared with that for acetone. The most striking feature is the close resemblance of both TCS energy dependences, with respect to the shape. Such likeness of TCSs, especially at the very low and intermediate energies where direct electron–dipole interactions dominate the scattering, is to some extent related to high (and nearly the same) electric dipole moments of both molecules (cf table 3). The replacement of the hydrogen atom in $(\text{CH}_3)\text{CHO}$ with the methylene group to form $(\text{CH}_3)_2\text{CO}$ increases the size of the resulting target molecule, what reflects in the increase of the TCS magnitude for acetone. Figure 3 shows that over a wide energy range, the TCS for $(\text{CH}_3)_2\text{CO}$ exceeds the one for $(\text{CH}_3)\text{CHO}$ with satisfactory accordance by a factor of 1.3. Only within the TCS enhancement, where numerous resonant processes become remarkable, the difference in the magnitude is distinctly higher. Based on this observation as well as on the correlation between

the intermediate-energy electron-scattering TCS and the gas-kinetic cross section, one can attempt to estimate σ_{gk} for acetaldehyde; it appears equal to $14\text{--}15 \times 10^{-20} \text{ m}^2$. It is worth noting that the TCS ratio (~ 1.3) for acetone and acetaldehyde is close to the ratio of their ionization cross sections that changes from 1.25 at 50 eV to 1.45 at 250 eV.

Finally, the cross sections between 1 and 2 eV need some comment; although, no TCS feature in this energy range can be directly discernible for acetaldehyde (figure 1) and only very subtle change of the TCS curve for acetone is noticeable in figure 2. For acetaldehyde, Naff *et al* (1972) and van Veen *et al* (1976)—in the threshold excitation spectra, van Veen *et al* (1976) and Jordan and Burrow (1978)—in the derivative of the transmitted electron current, Dressler and Allan (1986) and Benoit *et al* (1987)—in the vibrational excitation functions, observed the structure centred at 1.2–1.3 eV which has been ascribed to formation of the transient negative ion $(\text{CH}_3)\text{CHO}^-$ when the incoming electron is trapped into the lowest vacant molecular orbital, principally CO π^* in character. Van Veen *et al* (1976) revealed weak oscillations in the range of the resonant peak, which appeared to be (Benoit *et al* 1987) of the boomerang type (see Herzenberg 1968); this indicates that the auto-detachment lifetime of the $^2\pi^*$ resonant state is comparable to the period of nuclei oscillations in the acetaldehyde molecular anion. Unfortunately, all above-mentioned low-energy experiments do not give the magnitude of the resonant processes. Anyhow, the 1.2 eV resonance seems to be rather weak to manifest itself on the large and rapidly raising TCS background related to direct scattering processes.

For acetone, on the descending part of the TCS curve, between 1.2 and 2 eV, a weak change in the slope can be hardly discernible. The location of this feature coincides with the resonant structures already observed near 1.6 eV in the dissociative electron attachment spectra (Dorman 1966); the trapped electron spectra (Staley *et al* 1975); the transmission experiments (van Veen *et al* 1976, Jordan and Burrow 1978) and in the vibrational spectra taken by Benoit *et al* (1987). Also in this case, the intensities of the observed resonant features have been presented in relative units only. Lack of oscillatory structure in the excitation functions (Benoit *et al* 1987) suggests that the lifetime of the transient $(\text{CH}_3)_2\text{CO}^-$ anion is shorter than the period of nuclei oscillations. Note also, that a distinct shoulder is also visible near 1.6 eV in the TCS curve reported by Kimura *et al* (2000) and depicted in figure 2.

3.4. Comparison of electron-scattering TCSs for isomers of $\text{C}_2\text{H}_4\text{O}$ and $\text{C}_3\text{H}_6\text{O}$ compounds

Comparison between the TCSs for cyclic and open-chain isomers of the $\text{C}_2\text{H}_4\text{O}$ and $\text{C}_3\text{H}_6\text{O}$ compounds is shown in figures 4(a) and (b).

From figure 4(a), it is clearly seen that below 30–40 eV the compared TCSs for $\text{c}-(\text{CH}_2)_2\text{O}$ and $(\text{CH}_3)\text{CHO}$ differ in the magnitude and in shape, while above 50 eV they are not distinguishable in the limit of the experimental errors. Such TCS behaviour has been observed earlier for isomers of

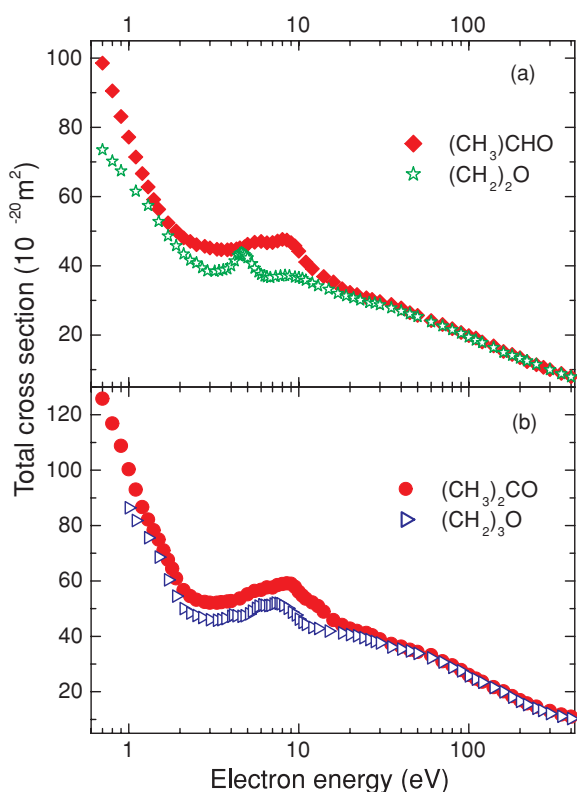


Figure 4. Comparison of total cross sections (TCSs) for electron scattering from isomers of $\text{C}_2\text{H}_4\text{O}$ and $\text{C}_3\text{H}_6\text{O}$ compounds. (a) $(\text{CH}_3)\text{CHO}$, present; and $c\text{-(CH}_2)_2\text{O}$, Szmytkowski *et al* (2008). (b) $(\text{CH}_3)_2\text{CO}$, present; and $c\text{-(CH}_2)_3\text{O}$, Szmytkowski *et al* (2009).

hydrocarbons (e.g. Szmytkowski and Kwitniewski 2002) and perfluorocarbons (Szmytkowski and Kwitniewski 2003). The rearrangement of atoms in the $\text{C}_2\text{H}_4\text{O}$ compound significantly disturbs symmetry of charge distribution in the resultant isomers. The open-chain $(\text{CH}_3)\text{CHO}$ isomer possesses much larger permanent electric dipole moment, 2.72 D, than its cyclic counterpart $c\text{-(CH}_2)_2\text{O}$, 1.89 D (cf table 3). In consequence, the difference of TCSs below 3 eV can be related to the substantial difference between long-range contributions to the electron–molecule interaction for both isomeric targets. Dissimilarity of these TCSs within 3–12 eV may be partly attributed to differences in the resonant scattering. While resonances in electron–acetaldehyde scattering seem to be mainly connected with the carbonyl group, $\text{C}=\text{O}$, in ethylene oxide they are predominantly related to CH_2 groups (Allan and Andric 1996). It leads to essential differences in the location and magnitude of resonant structures. Above 40–50 eV, the impinging electron sees the target molecule as a cluster of individual atoms rather than as a whole. Therefore, at intermediate and high electron-impact energies the charge distribution and/or arrangement of atoms in the molecule become less important and the independent atom approximation (Mott and Massey 1965) becomes valid.

Similar observations can be derived from figure 4(b) in which electron-scattering TCSs energy functions for acetylene and trimethylene oxide are compared. Again, below 3 eV, where TCS behaviour is determined by long-range electron–dipole interactions, the TCS for the open-chain $(\text{CH}_3)_2\text{CO}$

molecule of stronger dipole moment (2.88 D) is distinctly higher than the TCS for the cyclic $c\text{-(CH}_2)_2\text{O}$ isomer with the electric dipole moment of 1.94 eV (table 3). Differences in the 3–10 eV energy range can also be explained in terms of the resonant scattering. Above 40 eV TCSs for both isomers are the same in the magnitude and shape.

4. Concluding remarks

Absolute total cross sections for electron scattering from acetaldehyde and acetone have been measured at impact energies from 0.7 to 400 eV. The general shape of both obtained TCSs is typical for molecules of high permanent electric dipole moment. Below 2 eV, they decrease very steeply with energy increase due to long-range electron–dipole interactions; they have broad weak enhancements spanned between 4 and 12 eV which can be explained in terms of resonant effects; and above 10 eV they continuously fall down. TCS curves for $(\text{CH}_3)\text{CHO}$ and $(\text{CH}_3)_2\text{CO}$ appear to be very similar in the shape while the magnitude of TCS for acetone is over almost the whole energy range higher than that for acetaldehyde, by a factor of 1.3. Finally, the isomeric effect in TCS for $(\text{CH}_3)\text{CHO}$ and $(\text{CH}_3)_2\text{CO}$ and their cyclic counterparts $c\text{-(CH}_2)_2\text{O}$ and $c\text{-(CH}_2)_3\text{O}$, respectively, have been observed.

Acknowledgments

The author gratefully acknowledges the support by the Polish Government (MNSzW) research funds for 2008–2009.

References

- Allan M and Andric L 1996 *J. Chem. Phys.* **105** 3559–68
- Altshuler S 1957 *Phys. Rev.* **107** 114–7
- Benoit C, Abouaf R and Cvejanovic S 1987 *Chem. Phys.* **117** 295–304
- Beran J A and Kevan L 1969 *J. Phys. Chem.* **73** 3866–76
- Bull J N and Harland P W 2008 *Int. J. Mass Spectrom.* **273** 53–7
- Christophorou L G and Christodoulides A A 1969 *J. Phys. B: At. Mol. Phys.* **2** 71–85
- Christophorou L G and Olthoff J K 2004 *Fundamental Electron Interactions with Plasma Processing Gases* (Dordrecht: Kluwer)
- Crawford O H, Dalgarno A and Hays P B 1967 *Mol. Phys.* **13** 181–92
- Domaracka A, Mozejko P, Ptasinska-Denga E and Szmytkowski Cz 2006 *J. Phys. B: At. Mol. Opt. Phys.* **39** 4289–99
- Dorman F H 1966 *J. Chem. Phys.* **44** 3856–63
- Dressler R and Allan M 1985 *Chem. Phys. Lett.* **118** 93–6
- Dressler R and Allan M 1986 *J. Electron Spectrosc. Relat. Phenom.* **41** 275–87
- Field D 2005 *Europhys. News* **36** 51–5
- Garrett W R 1972 *Mol. Phys.* **24** 465–87
- Greenberg J M 2002 *Surf. Sci.* **500** 793–822
- Harrison A G, Jones E G, Gupta S K and Nagy G P 1966 *Can. J. Chem.* **44** 1967–73
- Herzenberg A 1968 *J. Phys. B: At. Mol. Phys.* **1** 548–58
- Huebner R H, Celotta R J, Mielczarek S R and Kuyatt C E 1973 *J. Chem. Phys.* **59** 5434–43
- Itikawa Y 2000–2003 (ed) *Photon and Electron Interactions with Atoms, Molecules and Ions* (Landoldt-Börnstein, vol 17A–C) (Berlin: Springer)
- Jordan K D and Burrow P D 1978 *Acc. Chem. Res.* **11** 341–8

- Kato C, Konaka S, Iijima T and Kimura M 1969 *Bull. Chem. Soc. Japan* **42** 2148–58
- Kato H, Makochekanwa C, Hoshino M and Tanaka H 2009 *Proc. of XXVI Int. Conf. on Photonic, Electronic and Atomic Collisions (Kalamazoo)* Abstracts Mo080
- Kimura M, Sueoka O, Hamada A and Itikawa Y 2000 *Adv. Chem. Phys.* **111** 537–622
- Knudsen M 1910 *Ann. Phys., Lpz.* **31** 205–29
- Lide D R (ed) 1995–1996 *CRC Handbook of Chemistry and Physics* 76th edn (Boca Raton, FL: CRC Press)
- Machado L E, Brescansin L M, Iga I and Lee M-T 2005 *Eur. Phys. J. D* **33** 193–9
- Miller K J 1990 *J. Am. Chem. Soc.* **112** 8533–42
- Mott N F and Massey H S W 1965 *The Theory of Atomic Collisions* (Oxford: Oxford University Press)
- Naff W T, Compton R N and Cooper C D 1972 *J. Chem. Phys.* **57** 1303–7
- Otvos J W and Stevenson D P 1956 *J. Am. Chem. Soc.* **78** 546–51
- Sanche L 2005 *Eur. J. Phys. D* **35** 367–90
- Silva H, Muse J, Lopes M C A and Khakoo M A 2008 *Phys. Rev. Lett.* **101** 033201
- Staley R H, Harding L B, Goddard W A III and Beauchamp J L 1975 *Chem. Phys. Lett.* **36** 589–93
- Stockdale J A D, Christophorou L G, Turner J E and Anderson V E 1967 *Phys. Lett. A* **25** 510–11
- Szmytkowski Cz, Domaracka A, Możejko P and Ptasińska-Denga E 2008 *J. Phys. B: At. Mol. Opt. Phys.* **41** 065204
- Szmytkowski Cz, Domaracka A, Możejko P and Ptasińska-Denga E 2009 *J. Chem. Phys.* **130** 134316
- Szmytkowski Cz and Kwitniewski S 2002 *J. Phys. B: At. Mol. Opt. Phys.* **35** 2613–23
- Szmytkowski Cz and Kwitniewski S 2003 *J. Phys. B: At. Mol. Opt. Phys.* **36** 4865–73
- Szmytkowski Cz, Możejko P and Kasperski G 1997 *J. Phys. B: At. Mol. Opt. Phys.* **30** 4363–72
- Szmytkowski Cz and Możejko P 2006 *Opt. Appl.* **36** 543–50
- Tam W-C and Brion C E 1974 *J. Electron Spectrosc. Relat. Phenom.* **3** 467–77
- van Veen E H, van Dijk W L and Brongersma H H 1976 *Chem. Phys.* **16** 337–45
- Walzl K N, Koerting C F and Kuppermann A 1987 *J. Chem. Phys.* **87** 3796–803